Size and Shape Characterization of Oblate Particles

W. PABST,[1] E. GREGOROVÁ,[1] C. BERTHOLD,[2] et al.

[1] Department of Glass and Ceramics, Institute of Chemical Technology, Prague, Czech Republic

[2] Institut für Geowissenschaften, Universität Tübingen, Germany

ICT PRAGUE

CPPS-Lecture
ad Units 5-7

Eberhard Karls Universität Tübingen

Introduction 1 – Sizing methods

The **most important sizing methods** used routinely for ceramic raw materials characterization are:

Laser diffraction (Mie / Fraunhofer approximation) – D_L
Sedimentation analysis (Stokes equation) – D_S
Microscopic image analysis – D_M

All these methods are based on **different physical principles** and thus measure **different equivalent diameters**. Only for spherical particles the sizing results coincide (calibration standards).

Introduction 2 – Oblate Particles

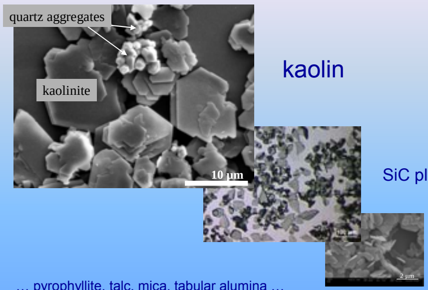

kaolin

SiC platelets

boron nitride

… pyrophyllite, talc, mica, tabular alumina …

Introduction 3 – Oblate particles

Particle size distributions measured via sedimentation analysis (Micromeritics Sedigraph 5100) and laser diffraction (Fritsch Analysette 22)

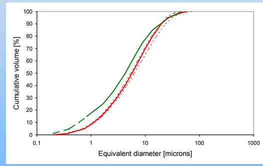

Low degree of anisometry (example pyrophyllite)

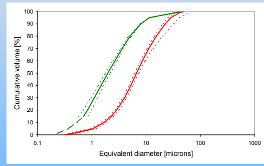

High degree of anisometry (example kaolin)

Introduction 4 – Oblate particles

Correlation of average particle shape and mineralogical phase composition in 5 commercial kaolin types from three different deposits (Czech Republic)

Kaolin type	D_{50}^{S} [µm]	D_{50}^{L} [µm]	Median LS shape factor
Sedlec Ia	1.3	5.9	48.4
Imperial / Premier	1.5	5.5	30.1
Sp-EX	2.9	8.0	17.9
KDG	2.4	5.0	10.3
KD50	7.7	11.8	5.6

Kaolin type	Kaolinite	Quartz	Feldspar	Other clay and mica minerals
Sedlec Ia	91 ± 3	2 ± 1	–	7 ± 2
Imperial / Premier	89 ± 4	3 ± 2	–	8 ± 3
Sp-EX	84	13	1	2
KDG	77 ± 4	13 ± 3	1 ± 1	9 ± 3
KD50	69 ± 4	23 ± 3	1 ± 1	7 ± 3

PABST et al.: *Brit. Ceram. Trans.* **100**, 106 (2001)

Introduction 5 – Oblate particles

Different average shape and quantitative phase composition in different size fractions of kaolins

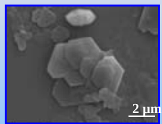

fraction
< 2 µm

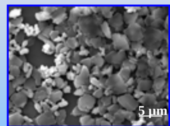

fraction
2 – 6.3 µm

fraction
6.3 – 20 µm

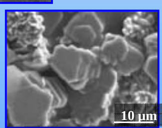

fraction
20 – 63 µm

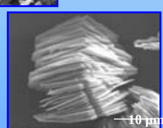

LEHMANN et al.: *Key Eng. Mater.* **264-268**, 1387 (2004)

Introduction 6 – Oblate particles

- Although most **real anisometric particles** have an **irregular** shape, many of them can **approximately** be considered as **rotationally symmetric**.
- The most convenient model shapes for **platelets** are **circular disks** and **oblate spheroids**.
- In this case shape can be characterized by a single number, the **aspect ratio**:

$$R \equiv \frac{D_M}{H}$$

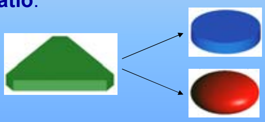

(maximum and minimum extension D_M – "diameter" and H – "height")

Theory 1 – Size distributions

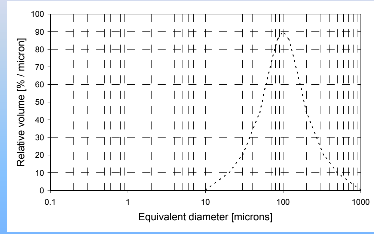

Theory 2 – Size distributions

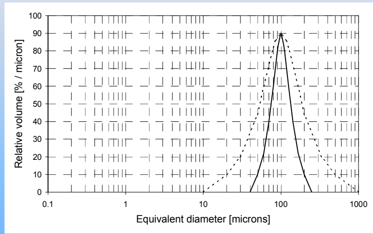

Theory 3 – Size distributions

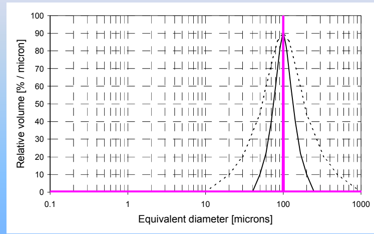

Theory 4 – Size distributions

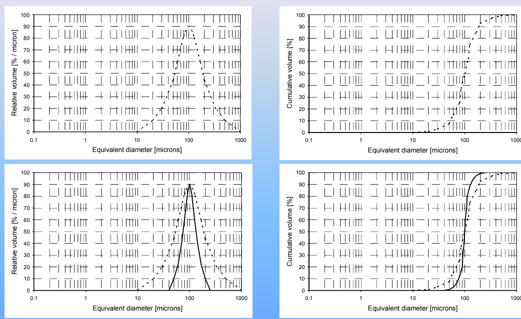

Theory 5 – Size distributions

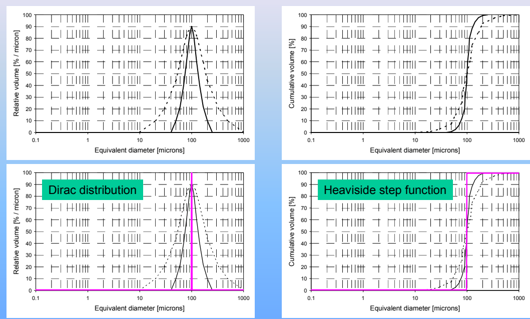

Theory 6 – Size distributions

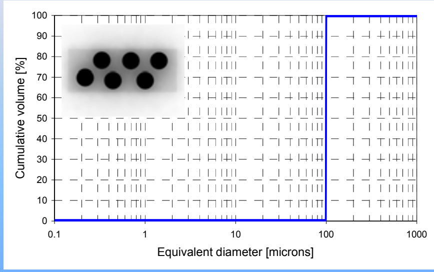

PABST, GREGOROVÁ, BERTHOLD et al.
ICT Prague (Czech Republic) & Universität Tübingen (Germany)

Theory 7 – Size distributions

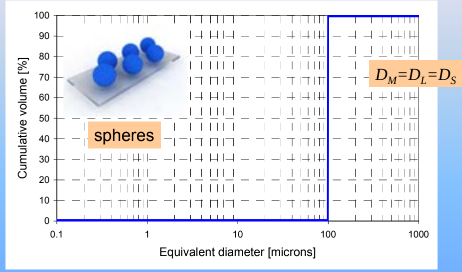

PABST, GREGOROVÁ, BERTHOLD et al.
ICT Prague (Czech Republic) & Universität Tübingen (Germany)

Theory 8 – Size distributions

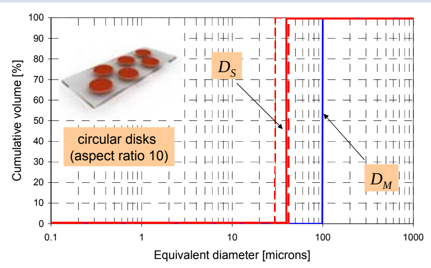

PABST, GREGOROVÁ, BERTHOLD et al.
ICT Prague (Czech Republic) & Universität Tübingen (Germany)

Theory 9 – Size distributions

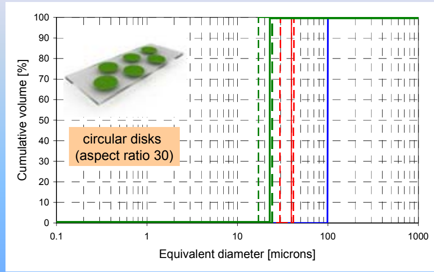

PABST, GREGOROVÁ, BERTHOLD et al.
ICT Prague (Czech Republic) & Universität Tübingen (Germany)

Theory 10 – Size distributions

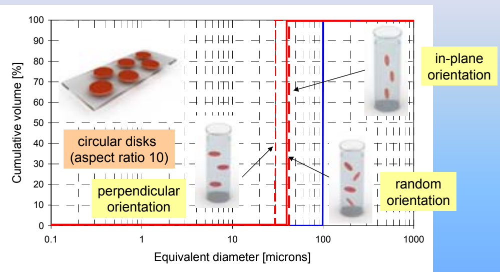

PABST, GREGOROVÁ, BERTHOLD et al.
ICT Prague (Czech Republic) & Universität Tübingen (Germany)

Theory 11 – Stokes equation

Classical Stokes equation for sedimentation analyses:

$$D_S = \sqrt{\frac{18\,\eta V}{(\rho_S - \rho_L)\,g}}$$

(dynamic shear viscosity η, steady-state settling velocity V, density of solid particles ρ_S and liquid ρ_L, gravitational acceleration g, **equivalent sphere diameter / Stokes diameter D_S**)

Derivation of the Stokes equation via force equilibrium:

$$\sum F = F_B - F_G + F_R = 0$$

$$F_B = \frac{\pi}{6} D_S^3 \rho_L\, g \qquad F_G = \frac{\pi}{6} D_S^3 \rho_S\, g \qquad F_R = 3\pi\,\eta V\, D_S$$

lift force (buoyancy) | gravitational force | resistance force

PABST, GREGOROVÁ, BERTHOLD et al.
ICT Prague (Czech Republic) & Universität Tübingen (Germany)

Theory 12 – Stokes equation

Modified Stokes equation for **circular disks**:

$$D_M = \sqrt{\frac{24\eta V R}{\pi(\rho_S - \rho_L) g}}$$

(dynamic shear viscosity η, steady-state settling velocity V, density of solid particles ρ_S and liquid ρ_L, gravitational acceleration g, **(equivalent) disk diameter D_M** and **aspect ratio R**)

Derivation of the Stokes equation via force equilibrium:

$$\sum F = F_B - F_G + F_R = 0$$

$$F_B = \frac{\pi}{4} \cdot \frac{D_M^3}{R} \rho_L g \qquad F_G = \frac{\pi}{4} \cdot \frac{D_M^3}{R} \rho_S g \qquad F_{R\,random} \approx 6 \eta V D_M$$

lift force (buoyancy) | gravitational force | resistance force

PABST, GREGOROVÁ, BERTHOLD et al.
ICT Prague (Czech Republic) & Universität Tübingen (Germany)

ICT PRAGUE

Theory 13 – Stokes equation

Modified Stokes equation for **oblate spheroids**:

$$D_M = \sqrt{\frac{36\eta V R}{\pi(\rho_S - \rho_L) g}}$$

(dynamic shear viscosity η, steady-state settling velocity V, density of solid particles ρ_S and liquid ρ_L, gravitational acceleration g, **(equivalent) spheroid diameter D_M** and **aspect ratio R**)

Derivation of the Stokes equation via force equilibrium:

$$\sum F = F_B - F_G + F_R = 0$$

$$F_B = \frac{\pi}{6} \cdot \frac{D_M^3}{R} \rho_L g \qquad F_G = \frac{\pi}{6} \cdot \frac{D_M^3}{R} \rho_S g \qquad F_{R\,random} \approx 6 \eta V D_M$$

lift force (buoyancy) | gravitational force | resistance force

PABST, GREGOROVÁ, BERTHOLD et al.
ICT Prague (Czech Republic) & Universität Tübingen (Germany)

ICT PRAGUE

Theory 14 – Aspect ratio formulae

- for **circular disks**: $R = \frac{3\pi}{4} \cdot \left(\frac{D_M}{D_S}\right)^2$

$$D_S = \sqrt{\frac{18\eta V}{(\rho_S - \rho_L) g}} \qquad D_M = \sqrt{\frac{24\eta V R}{\pi(\rho_S - \rho_L) g}}$$

(PABST et al.: *Brit. Ceram. Trans.* 2001, LEHMANN: M.Sc. Thesis (kaolins), Tübingen / Germany 2003, LOBATO: Ph.D. Thesis (on talc), Blacksburg / USA 2005)

- for **oblate spheroids**: $R = \frac{\pi}{2} \cdot \left(\frac{D_M}{D_S}\right)^2$

$$D_S = \sqrt{\frac{18\eta V}{(\rho_S - \rho_L) g}} \qquad D_M = \sqrt{\frac{36\eta V R}{\pi(\rho_S - \rho_L) g}}$$

D_S is the ordinary Stokes diameter (equivalent sphere diameter), D_M can be measured by image analysis.

PABST, GREGOROVÁ, BERTHOLD et al.
ICT Prague (Czech Republic) & Universität Tübingen (Germany)

ICT PRAGUE

Theory 15 – Aspect ratio formulae

In practice, these formulae are applied to compare sedimentation results with laser diffraction results (with the laser diffraction equivalent diameter D_L instead of the true disk or spheroid diameter D_M).

Problem: The shape factor (degree of anisometry) thus calculated can be called an aspect ratio only when the particles are oriented with their planes perpendicular to the laser beam direction.

Solution: When the particle orientation in the laser beam is random, Cauchy's stereological theorem has to be invoked to obtain the correct aspect ratio formula.

PABST, GREGOROVÁ, BERTHOLD et al.
ICT Prague (Czech Republic) & Universität Tübingen (Germany)

ICT PRAGUE

Theory 16 – Aspect ratio formulae

In the case of circular disks and oblate spheroids with large aspect ratio the surface area is approximately:

$$S \approx \frac{\pi}{2} \cdot D_M^2$$

Cauchy's stereological theorem says, that the average projected area of randomly oriented, monodisperse convex particles is just one quarter of the surface area of these particles.

$$A_{projection} = \frac{S}{4} \approx \frac{\pi}{8} \cdot D_M^2 \quad \Leftrightarrow \text{ laser diffraction: } \quad A_{projection} = \frac{\pi}{4} \cdot D_L^2$$

$\Rightarrow$ for large aspect ratios (approximately): $D_M \approx \sqrt{2} \cdot D_L$

PABST, GREGOROVÁ, BERTHOLD et al.
ICT Prague (Czech Republic) & Universität Tübingen (Germany)

ICT PRAGUE

Theory 17 – Aspect ratio formulae

	disks	spheroids	
oriented	$R = \frac{3\pi}{4} \cdot \left(\frac{D_M}{D_S}\right)^2$	$R = \frac{\pi}{2} \cdot \left(\frac{D_M}{D_S}\right)^2$	oriented
random	$R = \frac{3\pi}{2} \cdot \left(\frac{D_L}{D_S}\right)^2$	$R = \pi \cdot \left(\frac{D_L}{D_S}\right)^2$	random

PABST, GREGOROVÁ, BERTHOLD et al.
ICT Prague (Czech Republic) & Universität Tübingen (Germany)

ICT PRAGUE

Theory 18 – Aspect ratio formulae

Our simple aspect ratio formula for spheroids in random orientation, $R = \pi \cdot \left(\frac{D_L}{D_S} \right)^2$

can be considered as an approximation of the exact solution given by Jennings and Parslow (1988),

$$\frac{D_S}{D_L} = \sqrt{\frac{2R \arctan \sqrt{(R^2 - 1)}}{R\sqrt{(R^2-1)} + \ln\left[R + \sqrt{(R^2-1)}\right]}}$$

JENNINGS & PARSLOW: *Proc. Roy. Soc. London* **419**, 137 (1988)

because for large aspect ratios $R \to \infty$ we have

$\sqrt{(R^2 - 1)} \approx R$ $\qquad \frac{D_S}{D_L} = \sqrt{\frac{2R \arctan R}{R^2 + \ln 2R}}$ $\qquad \ln 2R << R^2$ $\qquad \arctan R \approx \pi/2$

PABST, GREGOROVÁ, BERTHOLD et al.
ICT Prague (Czech Republic) & Universität Tübingen (Germany)

Theory 19 – Aspect ratio formulae

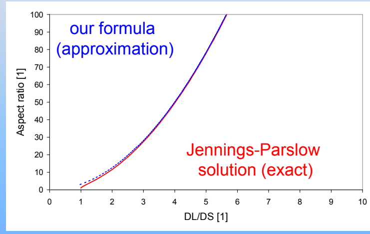

PABST, GREGOROVÁ, BERTHOLD et al.
ICT Prague (Czech Republic) & Universität Tübingen (Germany)

Theory 20 – Aspect ratio formulae

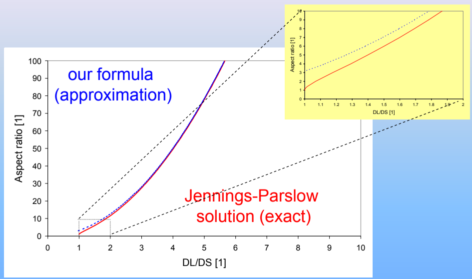

PABST, GREGOROVÁ, BERTHOLD et al.
ICT Prague (Czech Republic) & Universität Tübingen (Germany)

Theory 21 – Aspect ratio formulae

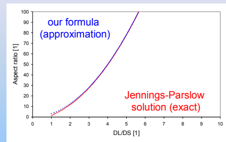

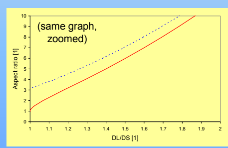

D_L / D_S	Jennings & Parslow	Our formula	Relative error [%]
1	1	3.140	214 %
1.1	2.301	3.799	65 %
1.2	3.195	4.522	42 %
1.3	4.088	5.307	30 %
1.4	5.013	6.154	23 %
1.5	5.984	7.065	18 %
1.6	7.005	8.038	15 %
1.7	8.081	9.075	12 %
1.8	**9.213**	**10.174**	**10 %**
1.9	10.403	11.335	9 %
2.0	11.652	12.560	8 %
2.2	14.331	15.198	6 %
2.4	**17.251**	**18.086**	**5 %**
2.6	20.418	21.226	4 %
2.8	23.831	24.618	3 %
3.0	27.492	28.260	3 %

PABST, GREGOROVÁ, BERTHOLD et al.
ICT Prague (Czech Republic) & Universität Tübingen (Germany)

Experimental 1 – SiC platelets

In practice, aspect ratio formulae are usually applied to sedimentation and laser diffraction results (D_S and D_L).

Key question: Are the particles randomly oriented during the laser diffraction experiment ?

Methodological approach to find the answer:
Perform a microscopic image analysis and find out whether coincidence with laser diffraction data can be achieved with or without the Cauchy theorem.

⇒ if coincidence is achieved only **with Cauchy** then the particle **orientation** in the laser beam is **random** !

PABST, GREGOROVÁ, BERTHOLD et al.
ICT Prague (Czech Republic) & Universität Tübingen (Germany)

Experimental 2 – SiC platelets

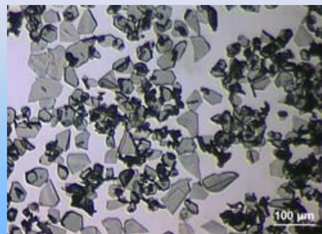

Optical micrograph of SiC platelets lying flatside on the object slide.

PABST, GREGOROVÁ, BERTHOLD et al.
ICT Prague (Czech Republic) & Universität Tübingen (Germany)

Experimental 3 – SiC platelets

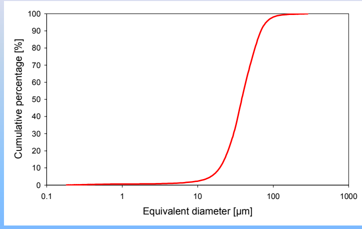

Cumulative size distribution of SiC platelets measured by laser diffraction.

PABST, GREGOROVÁ, BERTHOLD et al.
ICT Prague (Czech Republic) & Universität Tübingen (Germany)

Experimental 4 – SiC platelets

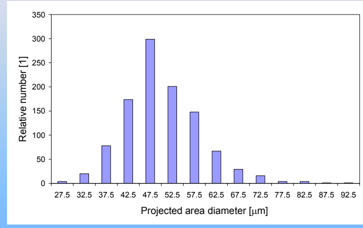

Number-weighted size distribution (frequency histogram of D_M).

PABST, GREGOROVÁ, BERTHOLD et al.
ICT Prague (Czech Republic) & Universität Tübingen (Germany)

Experimental 5 – SiC platelets

In order to transform the number-weighted (q_0) distribution to a volume-weighted distribution (q_3) via the equation

$$q_{3i} = R_i \cdot D_i^3 \cdot q_{0i}$$

the size dependence of the aspect ratio must be known.

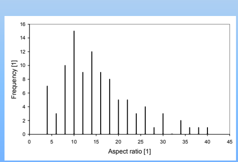

Frequency histogram of the aspect ratio.

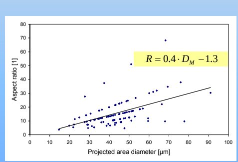

Size dependence of the aspect ratio.

PABST, GREGOROVÁ, BERTHOLD et al.
ICT Prague (Czech Republic) & Universität Tübingen (Germany)

Experimental 6 – SiC platelets

In order to transform the number-weighted (q_0) distribution to a volume-weighted distribution (q_3) via the equation

$$q_{3i} = R_i \cdot D_i^3 \cdot q_{0i}$$

the size dependence of the aspect ratio must be known.

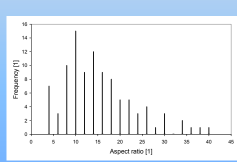

Frequency histogram of the aspect ratio.

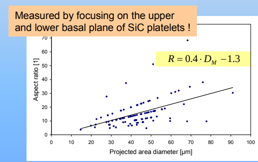

Size dependence of the aspect ratio.

PABST, GREGOROVÁ, BERTHOLD et al.
ICT Prague (Czech Republic) & Universität Tübingen (Germany)

Experimental 7 – SiC platelets

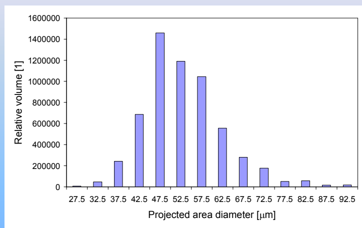

Volume-weighted size distribution obtained by transformation.

PABST, GREGOROVÁ, BERTHOLD et al.
ICT Prague (Czech Republic) & Universität Tübingen (Germany)

Experimental 8 – SiC platelets

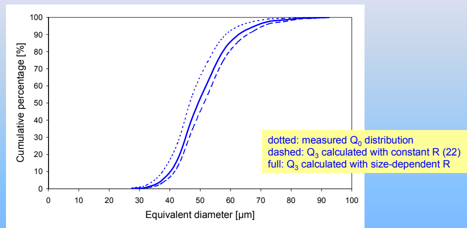

Cumulative size distribution of SiC platelets measured by image analysis.

PABST, GREGOROVÁ, BERTHOLD et al.
ICT Prague (Czech Republic) & Universität Tübingen (Germany)

Experimental 9 – SiC platelets

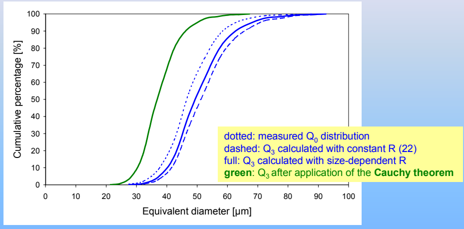

Size distribution of SiC platelets after applying the Cauchy theorem.

Experimental 10 – SiC platelets

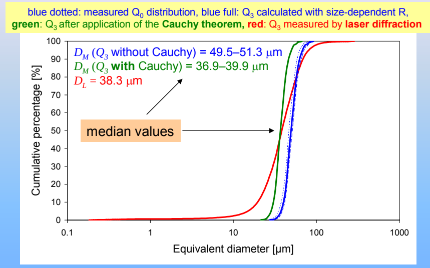

Comparison of size distributions of SiC platelets.

Summary and Conclusion – 1

- **New simple formulae** have been proposed to calculate the average aspect ratio of oblate particles when the size distribution is known from sedimentation analysis (D_S). and either microscopic image analysis (D_M) or laser diffraction (D_L). All of these approximate formulae are of the general form:

$$R = C \cdot K \cdot \left(\frac{D_M}{D_S} \right)^2 \qquad R = C \cdot K \cdot \left(\frac{D_L}{D_S} \right)^2$$

where the prefactor C (shape factor) is 3/2 for disks and 1 for spheroids and the prefactor K (orientation factor) is π/2 for perpendicular orientation (typically D_M) and π for random orientation (typically D_L).

Summary and Conclusion – 2

- **Our formula for randomly oriented spheroids**,

$$R = \pi \cdot \left(\frac{D_L}{D_S} \right)^2$$

is an approximation to the Parslow-Jennings solution,

$$\frac{D_S}{D_L} = \sqrt{\frac{2R \arctan \sqrt{(R^2 - 1)}}{R\sqrt{(R^2-1)} + \ln\left[R + \sqrt{(R^2-1)}\right]}}$$

for the case of large aspect ratios.

In practice, the error is < 10 % for aspect ratios > 10.

Summary and Conclusion – 3

- For SiC platelets it has been shown that after **application of Cauchy's sterological theorem** the size distribution measured by image analysis coincides well with the laser diffraction result:
  - median value of D_L: 38 µm,
  - median value of D_M without Cauchy: 49-51 µm,
  - median value of D_M with Cauchy: 37-40 µm.

⇒ SiC platelets are **randomly oriented** in the measuring cell of the laser diffraction instrument; this situation is **typical for laser diffraction**, unless special conditions are chosen / special equipment is used to enforce particle orientation.

X-ray and SEM studies of kaolins – 1

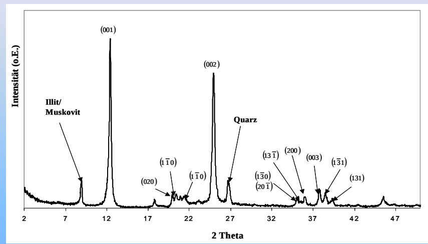

X-ray reflexes of kaolinite (example: kaolin Imperial, Czech Republic); note that the quartz main reflex (101) is at 26.41 ° 2θ, the illite / muscovite (001) and (002) reflexes are at 8.57 and 17.47 ° 2θ, respectively [Lehmann 2003].

X-ray and SEM studies of kaolins – 2

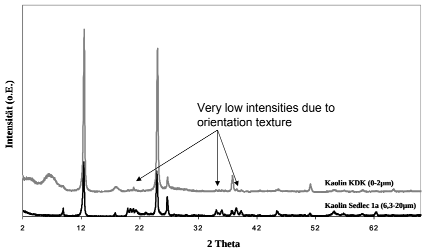

Influence of orientation texture on X-ray diffractograms (examples: kaolins KDK / Podbořany and Sedlec Ia, Karlovy Vary, Czech Republic): due to a higher degree of orientation some reflexes are suppressed in KDK [Lehmann 2003].

X-ray and SEM studies of kaolins – 3

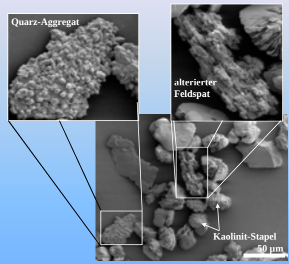

SEM micrographs of the coarse fraction of a kaolin (size fraction 20-63 µm of kaolin KD 50, Podbořany / Czech Republic) [Lehmann 2003].

PABST, GREGOROVÁ, BERTHOLD et al.
ICT Prague (Czech Republic) & Universität Tübingen (Germany)

X-ray and SEM studies of kaolins – 4

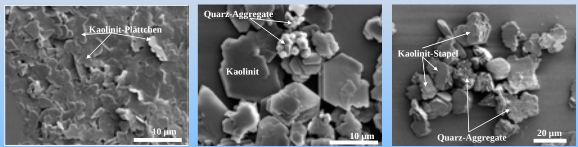

< 2 µm 2 – 6.3 µm 6.3 – 20 µm

SEM micrographs of different size fractions (< 2 µm, 2–6.3 µm and 6.3–20 µm) of **kaolin KD 50** (Podbořany / Czech Republic) [Lehmann 2003].

PABST, GREGOROVÁ, BERTHOLD et al.
ICT Prague (Czech Republic) & Universität Tübingen (Germany)

X-ray and SEM studies of kaolins – 5

< 2 µm

2–6.3 µm

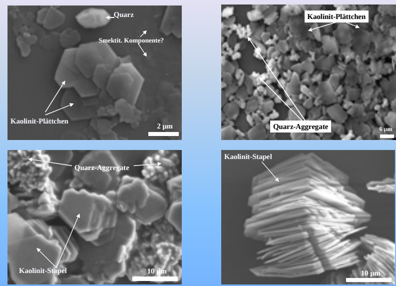

6.3–20 µm

20–63 µm

SEM micrographs of the different size fractions of **kaolin KDK** (Podbořany / Czech Republic) [Lehmann 2003].

PABST, GREGOROVÁ, BERTHOLD et al.
ICT Prague (Czech Republic) & Universität Tübingen (Germany)

X-ray and SEM studies of kaolins – 6

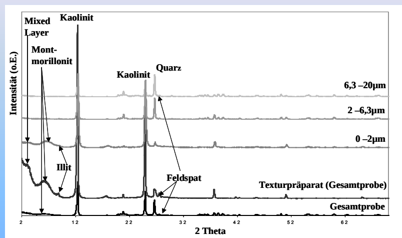

X-ray diffractograms of **kaolin KDK** (Podbořany, Czech Republic), total sample, textured sample and individual size fractions [Lehmann 2003].

PABST, GREGOROVÁ, BERTHOLD et al.
ICT Prague (Czech Republic) & Universität Tübingen (Germany)

X-ray and SEM studies of kaolins – 7

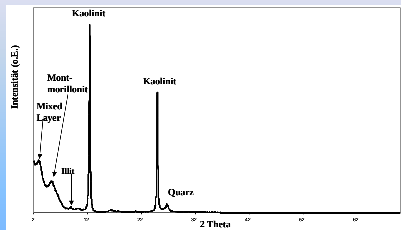

X-ray diffractogram of the fine size fraction (< 2 µm) of **kaolin KDK** (Podbořany, Czech Republic) **after swelling in glycol** (in order to emphasize the smectite and mixed layer minerals) [Lehmann 2003].

PABST, GREGOROVÁ, BERTHOLD et al.
ICT Prague (Czech Republic) & Universität Tübingen (Germany)

X-ray and SEM studies of kaolins – 8

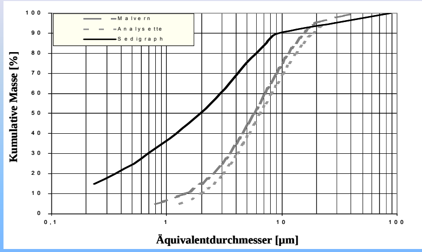

Particle size distributions of **kaolin KDK** (Podbořany, Czech Republic); comparison of sedimentation and laser diffraction results [Lehmann 2003].

Pabst, Gregorová, Berthold et al.
ICT Prague (Czech Republic) & Universität Tübingen (Germany)

ICT PRAGUE

X-ray and SEM studies of kaolins – 9

< 2 µm

2–6.3 µm

6.3–20 µm

20–63 µm

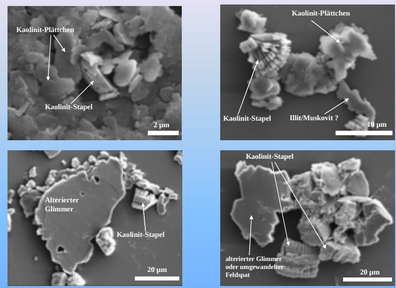

SEM micrographs of the different size fractions of **kaolin Imperial** (Karlovy Vary / Czech Republic) [Lehmann 2003].

Pabst, Gregorová, Berthold et al.
ICT Prague (Czech Republic) & Universität Tübingen (Germany)

ICT PRAGUE

X-ray and SEM studies of kaolins – 10

6.3–20 µm

20–63 µm

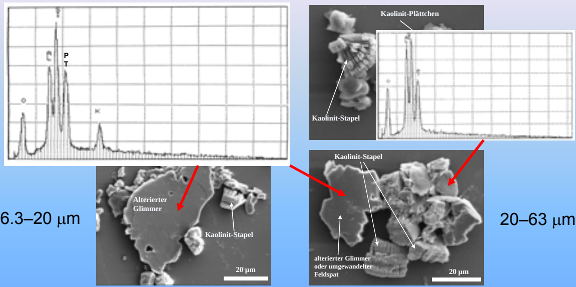

SEM and chemical analysis by EDX of single grains; note that the K-containing mineral could be mica or feldspar, cleavage suggests mica [Lehmann 2003].

Pabst, Gregorová, Berthold et al.
ICT Prague (Czech Republic) & Universität Tübingen (Germany)

ICT PRAGUE

X-ray and SEM studies of kaolins – 11

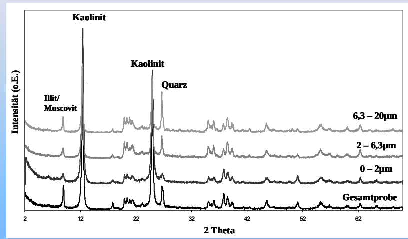

X-ray diffractograms of **kaolin Imperial** (Karlovy Vary, Czech Republic), total sample and individual size fractions [Lehmann 2003].

Pabst, Gregorová, Berthold et al.
ICT Prague (Czech Republic) & Universität Tübingen (Germany)

ICT PRAGUE

X-ray and SEM studies of kaolins – 12

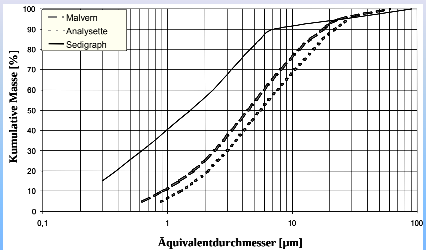

Particle size distributions of **kaolin Imperial** (Karlovy Vary, Czech Republic); comparison of sedimentation and laser diffraction results [Lehmann 2003].

Pabst, Gregorová, Berthold et al.
ICT Prague (Czech Republic) & Universität Tübingen (Germany)

ICT PRAGUE

X-ray and SEM studies of kaolins – 13

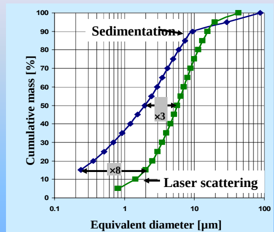

Typical **particle size distributions** of **kaolin**; (left h.s.: sedimentation, right h.s.: laser diffraction) [Lehmann et al. 2003].

Pabst, Gregorová, Berthold et al.
ICT Prague (Czech Republic) & Universität Tübingen (Germany)

ICT PRAGUE

X-ray and SEM studies of kaolins – 14

- Use of three different types of Czech kaolins: **Imperial®**, **KDK®** and **Sedlec 1a®**.
- Particle size analysis using laser diffraction (Malvern Mastersizer µ) and sedimentation (Micromeritics Sedigraph 5100).
- Separation of size fractions < 2µm, 2 – 6.3 µm, 6.3 – 20 µm and > 20 µm by sedimentation with Atterberg cylinders.
- Quantitative phase analysis (determination of mineral content) of whole sample as well as individual size fractions with XRD using the Rietveld-based software SIROQUANT®.

PABST, GREGOROVÁ, BERTHOLD et al.
ICT Prague (Czech Republic) & Universität Tübingen (Germany)

ICT PRAGUE

X-ray and SEM studies of kaolins – 15

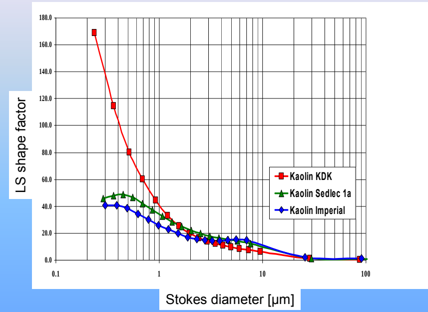

PABST, GREGOROVÁ, BERTHOLD et al.
ICT Prague (Czech Republic) & Universität Tübingen (Germany)

ICT PRAGUE

X-ray and SEM studies of kaolins – 16

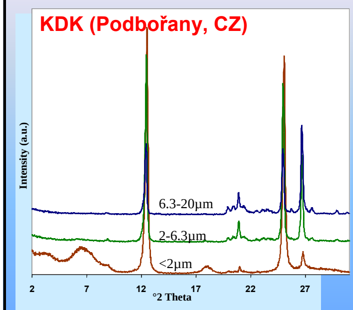

Mineral	Weight% Bulk sample	0 – 2 µm	2 – 6.3 µm	6.3 – 20 µm
Kaolinite	70	77	66	61
Quartz	18	8	26	27
Illite	2	4	1	3
Smectite/ ML	3	11	2	-
Feldspar	7	-	5	9

- High amounts of smectite / mixed-layer silicates in the fraction < 2 µm.
- Increasing quartz content with increasing grain size.

PABST, GREGOROVÁ, BERTHOLD et al.
ICT Prague (Czech Republic) & Universität Tübingen (Germany)

ICT PRAGUE

X-ray and SEM studies of kaolins – 17

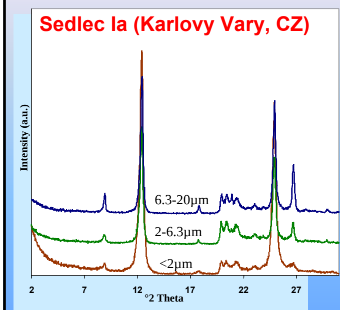

Mineral	Weight% Bulk sample	0 – 2 µm	2 – 6.3 µm	6.3 – 20 µm
Kaolinite	95	95	92	82
Quartz	2	2	3	12
Illite	3	3	5	6

- Increasing quartz content and decrasing kaolinite content with increasing grain size.

PABST, GREGOROVÁ, BERTHOLD et al.
ICT Prague (Czech Republic) & Universität Tübingen (Germany)

ICT PRAGUE

X-ray and SEM studies of kaolins – 18

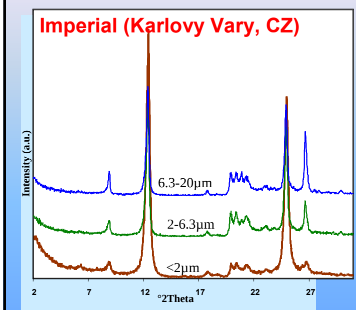

Mineral	Weight% Bulk sample	0 – 2 µm	2 – 6.3 µm	6.3 – 20 µm
Kaolinite	86	92	91	81
Quartz	5	2	5	10
Illite	8	5	4	9
Smectite	1	1	Detection limit	-

- Increasing quartz content with increasing grain size
- Increased mica (illite) content in the fraction 6.3 – 20 µm.

PABST, GREGOROVÁ, BERTHOLD et al.
ICT Prague (Czech Republic) & Universität Tübingen (Germany)

ICT PRAGUE

X-ray and SEM studies of kaolins – 19

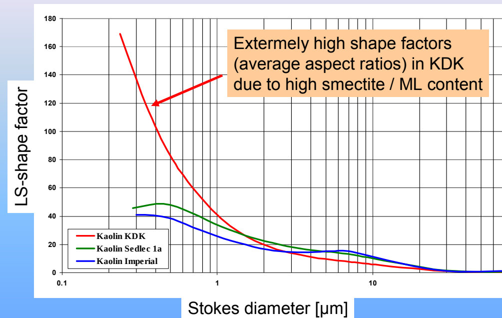

PABST, GREGOROVÁ, BERTHOLD et al.
ICT Prague (Czech Republic) & Universität Tübingen (Germany)

ICT PRAGUE

Acknowledgement

Bilateral Czech-German cooperation project D2-CZ21/06-07 “Characterization of Anisometric Particles and the Microstructure of Heterogeneous Materials”, DAAD (Germany) and **Academy of Sciences of the Czech Republic**, and research programme “Preparation and Research of Functional Materials and Material Technologies using Micro- and Nanoscopic Methods”, **Czech Ministry of Education, Youth and Sports** (Grant MSM 6046137302) and project “Tvorba předmětu Charakterizace částic a částicových soustav“, **Czech Ministry of Education, Youth and Sports** (Grant FRVŠ F1b 674).

The support is gratefully acknowledged.

Special thanks to M. Lehmann for his careful investigation of Czech kaolins,
T. Török for the creation of 3D figures,
J. Hostaša for calculating the statistic exercise problems
and many of our students for performing time-consuming measurements.

Acknowledgement

Selected references:

[1] Pabst W., Kuneš K., Havrda J., Gregorová E.: *J. Eur. Ceram. Soc.* **20** (2000), 1429.

[2] Pabst W., Kuneš K., Gregorová E., Havrda J.: *Brit. Ceram. Trans.* **100** (2001), 106.

[3] Pabst W., Kuneš K., Gregorová E., Havrda J.: *Key Eng. Mater.* **206-213** (2002), 743.

[4] Lehmann M.: Korngrössen- und Kornformcharakterisierung an Kaolinen (Grain size and shape characterization of kaolins, in German). M.Sc. Thesis, Universität Tübingen 2003.

[5] Lehmann M., Berthold C., Pabst W., Nickel K.G.: *Key Eng. Mater.* **264-268** (2004), 1387.

[6] Nováková M.: Velikostní a tvarová charakterizace destičkovitých částic (Size and shape characterization of oblate particles, in Czech). M.Sc. Thesis, ICT Prague 2007.

[7] Pabst W., Berthold C., Gregorová E.: *J. Eur. Ceram. Soc.* **27** (2007), 1759.

[8] Pabst W., Berthold C.: *Part. Part. Syst. Charact.* **24** (2007), 458.

PABST, GREGOROVÁ, BERTHOLD et al.
ICT Prague (Czech Republic) & Universität Tübingen (Germany)